J Membrane Biol (2009) 230:57–68
DOI 10.1007/s00232-009-9186-0

ORIGINAL ARTICLES

A Voltage-Dependent Ca^{2+} Influx Pathway Regulates the Ca^{2+}-Dependent Cl^- Conductance of Renal IMCD-3 Cells

John E. Linley · Stefan H. Boese · Nicholas L. Simmons · Michael A. Gray

Received: 26 February 2009 / Accepted: 11 June 2009 / Published online: 28 June 2009

Abstract We have previously shown that the membrane conductance of mIMCD-3 cells at a holding potential of 0 mV is dominated by a Ca^{2+}-dependent Cl^- current (I_{CLCA}). Here we report that I_{CLCA} activity is also voltage dependent and that this dependence on voltage is linked to the opening of a novel Al^{3+}-sensitive, voltage-dependent, Ca^{2+} influx pathway. Using whole-cell patch-clamp recordings at a physiological holding potential (−60 mV), I_{CLCA} was found to be inactive and resting currents were predominantly K^+ selective. However, membrane depolarization to 0 mV resulted in a slow, sigmoidal, activation of I_{CLCA} ($T_{0.5} \sim 500$ s), while repolarization in turn resulted in a monoexponential decay in I_{CLCA} ($T_{0.5} \sim 100$ s). The activation of I_{CLCA} by depolarization was reduced by lowering extracellular Ca^{2+} and completely inhibited by buffering cytosolic Ca^{2+} with EGTA, suggesting a role for Ca^{2+} influx in the activation of I_{CLCA}. However, raising bulk cytosolic Ca^{2+} at −60 mV did not produce sustained I_{CLCA} activity. Therefore I_{CLCA} is dependent on both an increase in intracellular Ca^{2+} and depolarization to be active. We further show that membrane depolarization is coupled to opening of a Ca^{2+} influx pathway that displays equal permeability to Ca^{2+} and Ba^{2+} ions and that is blocked by extracellular Al^{3+} and La^{3+}. Furthermore, Al^{3+} completely and reversibly inhibited depolarization-induced activation of I_{CLCA}, thereby directly linking Ca^{2+} influx to activation of I_{CLCA}. We speculate that during sustained membrane depolarization, calcium influx activates I_{CLCA} which functions to modulate NaCl transport across the apical membrane of IMCD cells.

Keywords Kidney · Collecting duct · Patch clamp · Calcium-dependent chloride current · Whole cell recording · Ca^{2+} influx channels

Electronic supplementary material The online version of this article (doi:10.1007/s00232-009-9186-0) contains supplementary material, which is available to authorized users.

J. E. Linley · N. L. Simmons · M. A. Gray (✉)
Epithelial Research Group, Institute for Cell and Molecular Biosciences, Medical School, Newcastle University, Newcastle upon Tyne NE2-4HH, UK
e-mail: m.a.gray@ncl.ac.uk

S. H. Boese
Zoophysiology, Institute for Biochemistry and Biology, University of Potsdam, Karl-Liebknecht-Str. 24-25, 14476 Potsdam, Germany

Present Address:
J. E. Linley
Institute of Membrane and Systems Biology, University of Leeds, Leeds LS2-9JT, UK

Present Address:
S. H. Boese
CECAD Cologne - Excellent in Aging Research, University of Cologne, Zülpicher Str. 47, 50674 Cologne, Germany

The renal inner medullary collecting duct (IMCD) is the final site of tubular filtrate modification and has the capacity for both net NaCl absorption and secretion, depending on the prevailing physiological state (Rocha and Kudo 1990; Wallace et al. 2001). Using whole-cell patch-clamp current recordings at a holding potential of 0 mV, we have previously shown that the dominant membrane conductance of mIMCD-3 cells (a model of the terminal portion of the IMCD) is due to an outwardly rectifying, time-independent, calcium-dependent Cl^- current (I_{CLCA}) (Shindo et al. 1996; Stewart et al. 2001; Linley et al 2007). We have demonstrated that this conductance is acutely regulated by changes in extracellular calcium concentration as well as by increases in cytosolic Ca^{2+} brought about by $G_{q/11}$-coupled

receptor agonists such as ATP and extracellular zinc (Stewart et al. 2001; Linley et al. 2007). $G_{q/11}$-coupled receptor agonists also stimulate transepithelial Cl^- secretion in polarized monolayers of mouse mIMCD-3 cells under short circuit conditions (Kose et al. 1997). An interesting aspect of I_{CLCA} in mIMCD-3 cells is that the current does not display the intermediate time- and voltage-dependent kinetic properties and rapid response to intracellular calcium seen for canonical calcium-activated Cl^- conductances in many epithelial cells, including some other collecting duct cell lines (Evans and Marty 1986; Bertog et al. 1999; Boese et al. 2000, 2004). Indeed, the unusually large magnitude of I_{CLCA} in mIMCD-3 cells measured under resting conditions at holding potentials of 0 mV, together with its regulation by external calcium levels, has suggested a working hypothesis in which a Ca^{2+} influx pathway in mIMCD-3 cells is responsible for maintaining I_{CLCA} active by establishing a raised calcium level in a near-membrane domain. In collecting duct cells changes in intracellular calcium are an important determinant of duct cell function (Kose et al. 2000; Stewart et al. 2001; Linley et al. 2007), but the identity of the pathways responsible for calcium entry and homeostasis in the IMCD are poorly understood (Magaldi et al. 1989; Hoenderop et al. 2005).

There are a number of potential molecular candidates for the putative Ca^{2+} influx pathway based on mRNA and/or functional studies in IMCD cells. These include several members of the TRP superfamily, TRPV5/6 and TRPP2 (Pazour et al. 2002; Nijenhuis et al. 2003; Hoenderop et al. 2005; Yoder 2007), as well as L- and T-type Ca^{2+} channels (Andreasen et al. 2000; Zhao et al. 2002). In this report we provide evidence for a novel regulatory mechanism of I_{CLCA} in mIMCD-3 cells. We show that activation of I_{CLCA} required prolonged membrane depolarization, whereas hyperpolarization reversed this process. The depolarization-induced activation of I_{CLCA} was absolutely dependent on, and preceded by, Ca^{2+} influx through a voltage-dependent Ca^{2+} permeable pathway. This influx pathway was equally permeable to Ca^{2+} and Ba^{2+} and was inhibited by Al^{3+}, Gd^{3+} and La^{3+}, but not verapamil. These results therefore provide strong evidence to support our hypothesis that Ca^{2+} influx is required to maintain I_{CLCA} active in mIMCD-3 cells under depolarized conditions. The possible molecular nature of the Ca^{2+} influx pathway and its physiological relevance to Cl^- transport in IMCD cells are discussed.

Methods

Cell Culture

mIMCD-3 cells (Rauchman et al. 1993; Vandewalle et al. 1999) were grown in 75-cm^2 Roux flasks without antibiotics in Hams F12 and DMEM (50/50%, v/v) with 1 g/l glucose, 10% fetal calf serum, and 2 mM L-glutamine at 37°C in humidified air:5% CO_2 (Shindo et al. 1996; Stewart et al. 2001). For patch-clamp experiments, mIMCD-3 were seeded on 24-mm glass coverslips in six-well culture plates at a density of 2,200–11,000 cells/cm^2 and used 1 to 5 days later.

Patch-Clamp Recording

Current recordings were mainly made using the perforated patch or "slow" whole-cell recording technique and employed amphotericin B (240 μg/ml) or Nystatin (100–300 mg/ml) as the pore forming antibiotic. In some experiments fast whole-cell recordings were made using conventional methods (Shindo et al. 1996). Currents were amplified using an EPC-7 or EPC-9 patch-clamp amplifier (HEKA Electronics, Lambrecht, Germany), filtered at 1 kHz by an eight-pole Bessel filter, then digitized at a sampling rate of 2 kHz (EPC-7—CED 1401, UK; EPC-9—ITC-16, InstruTECH, USA). Steady-state current/voltage (I/V) relationships were measured by applying 500-ms voltage pulses from V_{hold} to potentials between ±100 mV in 20-mV steps. The change in whole-cell current with time was monitored by applying a 500-ms voltage pulse from −60 to +60 mV every 10 s or from 0 to ±60 mV every 10 s. Series resistance and liquid junction potentials were corrected for as previously described (Stewart et al. 2001). Whole-cell currents were calculated at the reversal potential (E_{rev}) ± 60 mV, normalized to cell capacitance measured using the EPC-7/9 circuitry, and are expressed as pA/pF. Relative ion permeabilities were calculated from the shift in E_{rev} upon changing of the bath ion concentration using the Hodgkin-Katz modification of the Goldman equation. In order to substantiate depolarization activation of an inward, Ca^{2+}-selective current, cell membrane current in perforated patch recordings were clamped to zero (in current clamp mode) and the resulting membrane potential (V_m) was measured. Replacement of the standard Na-rich bath solution (see below) with the standard pipette solution ($KCl_{in} = KCl_{out}$) plus 1 mM $CaCl_2$ at zero holding current should result in a membrane potential shift to ~0 mV if no Ca^{2+} conductance is present or activated. Rates of activation of I_{CLCA} by voltage were calculated from the slope of the linear phase of activation and are expressed as the change in current density at +60 mV with time, (pA/pF)/s.

Solutions and Chemicals

The standard bathing solution for patch-clamp experiments contained (mM) 137 NaCl, 5.4 KCl, 2.8 $CaCl_2$, 1.2 $MgCl_2$, 0.3 NaH_2PO_4, 0.3 KH_2PO_4, 14 TRIS, and 5 glucose and

was titrated to pH 7.4 with HCl. For ion selectivity experiments, 100 mM NaCl was replaced with an osmotic equivalent of mannitol, *N*-methyl-D-glucamine Cl, or KCl. The standard pipette solution contained (mM) 130 KCl, 10 NaCl, 2 $MgCl_2$, and 10 Hepes, titrated to pH 7.4, with NaOH. Amphotericin/Nystatin was added from a DMSO stock to give a final concentration of 240 μg/ml or 100–300 mg/ml, respectively. For fast whole-cell recording, TEA-Cl replaced KCl and 1 mM ATP was present. In current-clamp experiments the standard pipette solution was used to replace the standard bathing solution, except that total calcium was increased to 1.0 mM. In experiments investigating divalent cation selectivity, all $CaCl_2$ was removed and replaced by the appropriate divalent (barium, manganese, or strontium) Cl^-salt. For nominally calcium-free bath solutions, $CaCl_2$ was simply omitted. $AlCl_3$ was added directly to bath solutions prior to pH adjustment, but generation of HCl required additional base to bring this solution pH to 7.4.

Statistics

Data are expressed as the mean ± SE for *n* experiments. Statistical comparisons were performed using ANOVA with Bonferroni posttests for multiple comparisons.

Results

I_{CLCA} Is Regulated by Membrane Depolarization

Figure 1 demonstrates that I_{CLCA}, the large Ca^{2+}-dependent Cl^-conductance, of mIMCD-3 cells (Shindo et al. 1996; Stewart et al. 2001; Linley et al. 2007) is regulated by membrane voltage. When the cell was held mainly at a physiological membrane potential of −60 mV (with only brief excursions to +60 mV), steady-state currents were small, outwardly rectifying, and moderately time dependent at membrane potentials ≥ +80 mV (Fig. 1B[a]). Ion substitution experiments at −60 mV showed this basal conductance to have a high selectivity for K^+ over Cl^- (see Supplementary Fig. S1; mean shift in reversal potential when changing from a NaCl-rich to a KCl-rich bath = +32 ± 5 mV, $n = 8$; mean shift in reversal potential when replacing 100 mM bath NaCl with mannitol = +2 ± 5 mV, $n = 5$). In marked contrast, when the membrane potential was held mainly at 0 mV, with only brief excursions to ±60 mV, there was a progressive increase in whole-cell conductance following a delay/slow activation phase of ~60 s (Fig. 1A). Under these conditions whole-cell currents at +60 mV increased by approximately sixfold, from 31 ± 3 pA/pF (V_{hold} = −60 mV) to 214 ± 22 pA/pF (V_{hold} = 0 mV) (paired *t*-test, $n = 37$, $P < 0.001$), reaching a plateau after ~15 min. A similar increase in the current at −60 mV was also observed (−18 ± 2 pA/pF at V_{hold} = −60 mV; −109 ± 9 pA/pF at V_{hold} = 0 mV) (paired *t*-test, $n = 37$, $P < 0.001$). Whole-cell currents under depolarized conditions were outwardly rectifying but time independent (Fig. 1B[b]). The increase in whole-cell conductance was accompanied by a shift in reversal potential (E_{rev}) toward the chloride equilibrium potential (from −26 ± 1 to −13 ± 1 mV), indicating that the activated conductance was now predominately Cl^- selective (paired *t*-test, $n = 37$, $P < 0.001$). This was confirmed by replacement of bath NaCl (100 mM) by mannitol, which gave a shift in reversal potential of 17 ± 2 mV ($n = 10$). The properties of this voltage-activated conductance are identical to those we have previously described for I_{CLCA} in mIMCD-3 cells (Shindo et al. 1996; Stewart et al. 2001). Therefore, membrane depolarization to 0 mV was associated with a marked change in resting cell Cl^- permeability.

Upon return of the holding potential to −60 from 0 mV, there was a relatively rapid decrease in I_{CLCA} to prestimulation levels, indicating that the effect of membrane depolarization was completely reversible (Fig. 1A). However, an interesting feature of the response of I_{CLCA} to changes in membrane potential was the difference in kinetics between activation and deactivation; deactivation was well described by a monoexponential decay, with a $T_{0.5}$ of 90 ± 10 s ($n = 15$), compared to activation, which showed more complex kinetics. Here the activation process, after the shift to 0 mV, showed a sigmoidal type of response, with a slowly activating (lag) period followed by an increase in current, with the much longer $T_{0.5}$ (time to 50% of plateau) of 472 ± 23 s ($n = 26$). The difference in the activation/deactivation kinetics was maintained during multiple activation/deactivation cycles in the same cell (illustrated in Fig. 5A).

The effect of holding potential on steady-state levels of I_{CLCA} was investigated further by monitoring the response of the cells to incremental depolarizing steps from an initial holding potential of −80 mV (Fig. 2). Stepwise depolarizations to holding potentials of −60, −40, −20, and 0 mV resulted in incremental increases in whole-cell current that reached steady state within 600 s of changing the holding potential (measured at ±60 mV). Depolarization resulted in a significant rise in the whole-cell current at +60 mV when the holding potential was depolarized past −40 mV (−80 vs. −20 mV, $P < 0.01$; −80 vs. 0 mV, $P < 0.001$).

These results suggested that membrane depolarization was linked to a slow activation of I_{CLCA}, and we suspected that this was due to the entry of Ca^{2+} through voltage-sensitive channels. To test for this an identical voltage protocol was utilized but Ca^{2+} in the external solution was reduced. Note that we could not eliminate Ca^{2+} from the

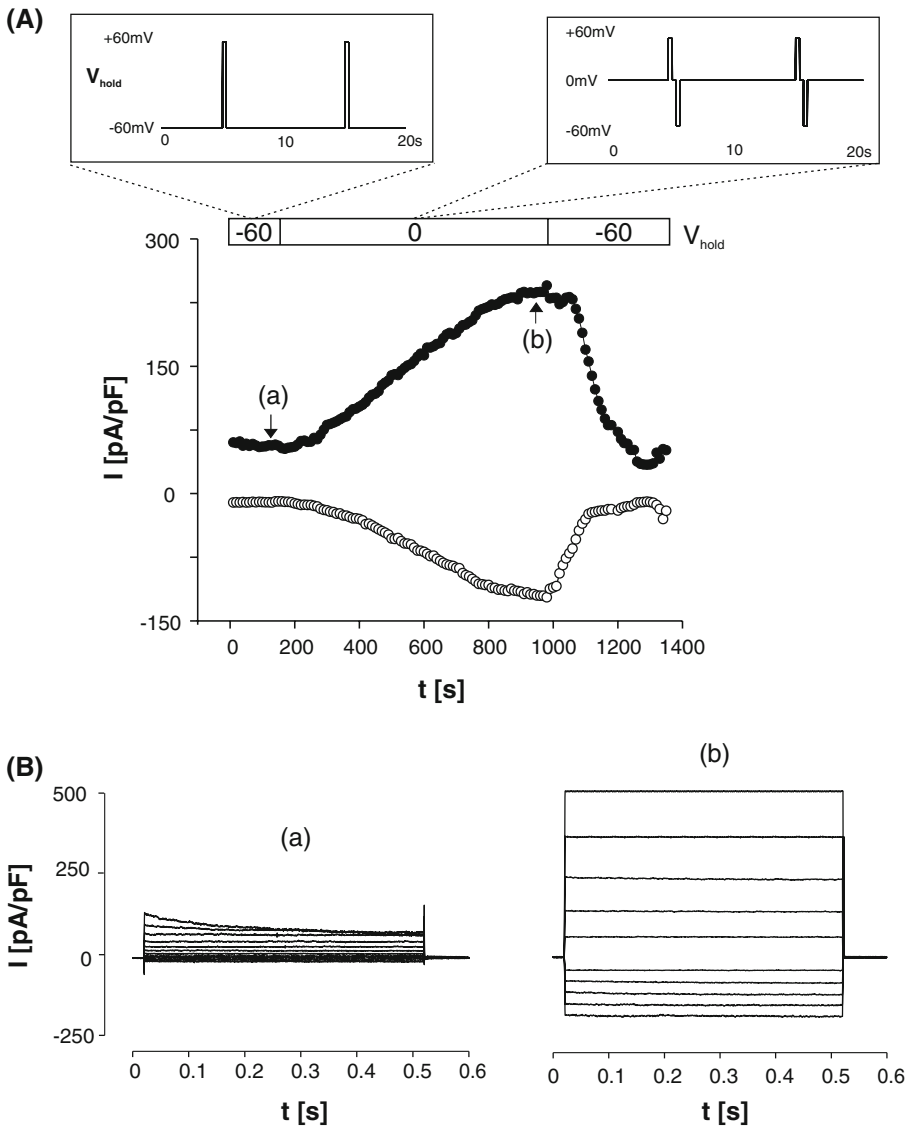

Fig. 1 I_{CLCA} is activated by cell depolarization and deactivated by hyperpolarization in mIMCD-3 cells. **A** Using the perforated whole-cell patch-clamp technique, the current at +60 mV (●) and −60 mV (○) was plotted in response to changing V_{hold} (see insets). **B** Steady-state current traces obtained by 500-ms voltage pulses from V_{hold} to ±100 mV in 20-mV steps taken at (a) $V_{hold} = -60$ mV and (b) $V_{hold} = 0$ mV

perfusion solution (e.g., by adding EGTA), because this led to the activation of a large cation-selective conductance in these cells (Stewart et al. 2001). However, using a nominally Ca^{2+}-free bathing solution (free activity ~47 nM [Linley et al. 2007]), changing the holding potential from −60 to 0 mV still resulted in activation of the I_{CLCA} (Fig. 3A). However, the rate of activation (2.8 mM Ca^{2+}, 0.22 ± 0.06 pA/pF/s; nominally Ca^{2+} free, 0.11 ± 0.01 pA/pF/s; unpaired *t*-test, $n = 7$, $P < 0.05$) and the mean steady-state current were significantly lower than in controls conducted in the presence of normal calcium levels (2.8 mM Ca^{2+}, 232 ± 29 and −133 ± 18 pA/pF; nominally Ca^{2+} free, 139 ± 32 and −76 ± 15 pA/pF; unpaired *t*-test, $n = 7$, $P < 0.05$) (Fig. 3A). Note that when the holding potential was returned to −60 mV, I_{CLCA} deactivated normally and within a time frame similar to that seen in calcium-containing solutions. Most calcium channels are also permeable to barium ions (Bean 1989). Repeating experiments where bath calcium (2.8 mM) was completely replaced with barium produced identical results in terms of the rate (control [Ca^{2+} present], 0.31 ± 0.12 pA/pF/s; Ba^{2+} replacement, 0.34 ± 0.08 pA/pF/s; $n = 4$, $P =$ ns) and the extent of activation of I_{CLCA} (control [Ca^{2+} present], 180 ± 24 pA/pF; Ba^{2+} replacement, 227 ± 17 pA/pF; $n = 4$, $P =$ ns). These results provide further support that depolarization leads to opening of calcium-selective channels in mIMCD-3 cells and that Ba^{2+} ions can substitute for Ca^{2+} in the activation of I_{CLCA}.

To test this further we reasoned that increasing the calcium buffering capacity of the mIMCD-3 cells should also eliminate the activation of I_{CLCA}. Figure 3B shows additional experiments using the standard or fast whole-

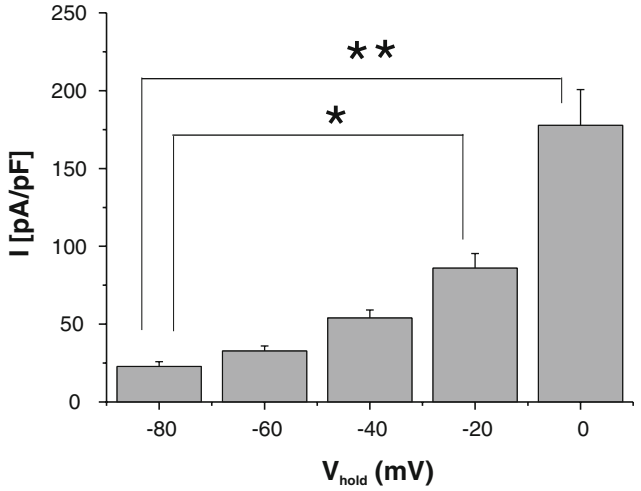

Fig. 2 Summary of the effect of membrane holding potential on the magnitude of whole-cell currents in mIMCD-3 cells. Membrane potential (V_{hold}) was held predominantly at the indicated voltage and steady-state current density measured after 15 min at $E_{rev} = +60$ mV. Data expressed as mean ± SE; n = 6–11. Data at 0 and −20 mV significantly different from data at −80 mV; $P < 0.001$ and $P < 0.01$, respectively

cell recording configuration, employing a pipette solution containing a high concentration of the diffusible Ca^{2+} chelator EGTA (5 mM). In this case the steady-state currents at a holding potential of −60 mV were small and the resulting IV relationship linear, with a current density of 10 ± 2 and −10 ± 2 pA/pF ($n = 8$), comparable to the currents recorded in the perforated patch experiments (see above). However, when the holding potential was then changed from −60 to 0 mV, no significant increase in current density was observed ($n = 8$). Note that this finding contrasts with our previous experiments using a lower pipette EGTA concentration (0.2 mM), in which holding the membrane potential at 0 mV did lead to substantial I_{CLCA} activity (Shindo et al. 1996).

To test further whether the membrane potential led indirectly to the activation of I_{CLCA}, both the holding potential and the intracellular Ca^{2+} concentration were varied. Using the fast whole-cell technique, the intracellular Ca^{2+} concentration was fixed and the membrane potential clamped to either −60 or 0 mV (Fig. 4). With the membrane potential clamped predominantly at −60 mV,

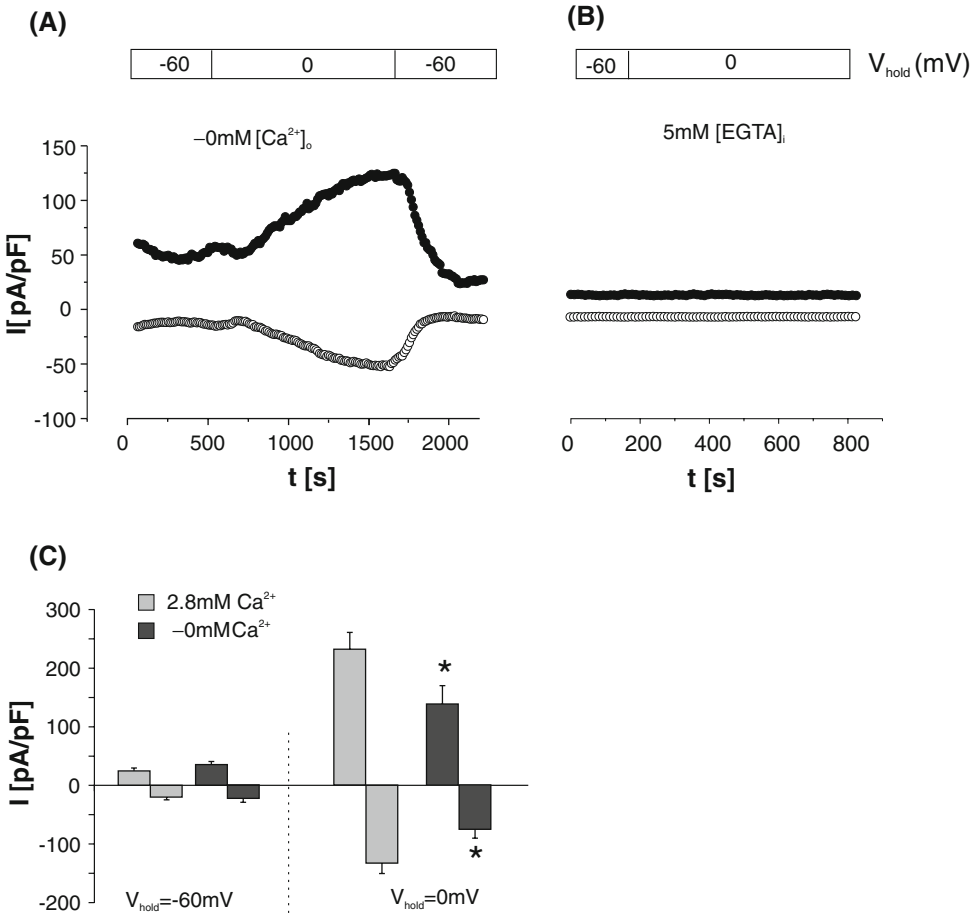

Fig. 3 Activation of I_{CLCA} by depolarization is Ca^{2+} dependent. Whole-cell patch-clamp recording from mIMCD-3 cells illustrating the Ca^{2+} dependence of the depolarization-induced activation of I_{CLCA}. **A** Perforated whole-cell patch-clamp recording. Current at +60 mV (●) and −60 mV (○) is plotted with a nominally Ca^{2+}-free bathing solution in response to change of the membrane holding potential (V_{hold}) as indicated by the upper bar. **B** Conventional fast whole-cell recording with EGTA (5 mM) introduced into the cell cytosol through the patch pipette. **C** Mean results from A are expressed as current density measured at $E_{rev} = +60$ mV (upper columns) and $E_{rev} = -60$ mV (lower columns). *Significant difference between the groups at $V_{hold} = 0$ mV (unpaired t-test; n = 7; $P < 0.05$). Shading of bars indicates the bath Ca^{2+} concentration

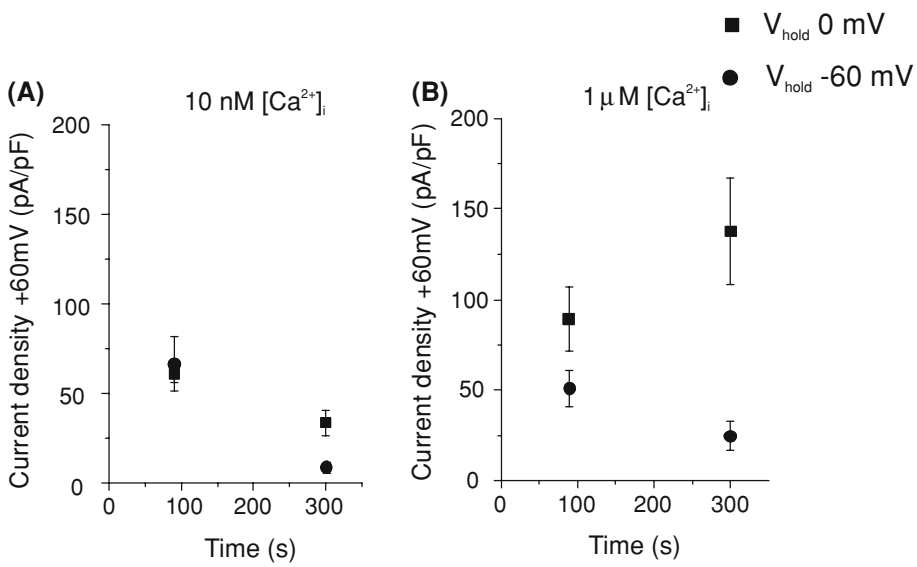

Fig. 4 Voltage and Ca^{2+} sensitivity of I_{CLCA}. Using the fast whole-cell patch-clamp technique, $[Ca^{2+}]_i$ was buffered to either 10 nM (**A**) or 1 μM (**B**), and the current density at +60 mV plotted. Data represent mean ± SE (A, $n = 13$; B, $n = 14$). Note that both membrane depolarization and elevated cytosolic Ca^{2+} were required to maintain I_{CLCA} activity

and $[Ca^{2+}]_i$ buffered to either 10 nM or 1 μM, I_{CLCA} activated transiently upon achieving the whole-cell configuration, however, the current then rapidly declined, reaching a steady-state current level which displayed a linear IV relationship. Similar rundown was observed with the membrane potential held predominantly at 0 mV with $[Ca^{2+}]_i$ fixed to 10 nM (5 mM EGTA), indicating that depolarization alone was insufficient for sustained I_{CLCA} activity. However, when Ca^{2+} was elevated to 1 μM in combination with a holding potential of 0 mV, I_{CLCA} currents did not display significant rundown. Taken together these data demonstrate that both depolarization and Ca^{2+} are required for sustained activation of I_{CLCA}.

Pharmacological Sensitivity of the Calcium Influx Pathway

We used a pharmacological approach to try and identify the putative Ca^{2+} influx pathway in mIMCD-3 cells. To investigate the contribution of voltage-sensitive L-type Ca^{2+} channels, verapamil (10 μM) was included in the bath solution prior to the change in the holding potential from −60 to 0 mV. Despite the presence of verapamil, depolarization was still accompanied by an increase in the whole-cell current, which reached a plateau of 173 ± 20 and −86 ± 6 pA/pF when measured at ±60 mV, over a similar time course compared to controls (Supplementary Fig. S2). The steady-state currents displayed kinetics identical to I_{CLCA} activated in the absence of drug and were not significantly different in magnitude from controls (150 ± 22 and −78 ± 16; unpaired *t*-test, $n = 3$, $P =$ ns). Verapamil at an elevated dose (32 μM) was also without effect on fully activated I_{CLCA} under depolarized conditions (88 ± 18% of the values at +60 mV; $n = 3$, $P =$ ns). Furthermore, using Fura-2-loaded cells to monitor intracellular Ca^{2+} levels (Shindo et al. 1996; Linley et al. 2007), addition of the L-type Ca^{2+} channel agonist, Bay-K 8644 (1 μM), had no effect on bulk cytosolic Ca^{2+} levels despite these cells displaying a normal extracellular ATP-mediated increase in cytosolic Ca^{2+} (Supplementary Fig. S2D). Interestingly, no increase in bulk cytosolic Ca^{2+} was observed upon membrane depolarization (induced by high bath KCl; Supplementary Fig. S3), suggesting that any calcium entry into the cell is limited to a region close to the plasma membrane.

We next tested the effect of Al^{3+}, which has previously been shown to block voltage-gated calcium channels in several different neuronal preparations (Busselburg et al. 1994; Bobkov and Ache 2005), as well as calcium influx mediated by AtTPC1 when expressed in plant cells (Kawano et al. 2004; Lin et al. 2005). Figure 5A shows that Al^{3+} (1 mM) was without effect on basal whole-cell currents at −60 mV, however, the presence of Al^{3+} completely abolished the activation of I_{CLCA} when the holding potential was switched to 0 mV. The effect of Al^{3+} was fully reversible on washout of the cation (with holding potential maintained at 0 mV). Of particular note in these experiments is that I_{CLCA} activated very quickly upon washout of Al^{3+} (Fig. 5A), with a time constant $T_{0.5}$ of ~110 s, which contrasts markedly with the slow activation of I_{CLCA} in the absence of Al^{3+} ($T_{0.5}$ ~ 470 s). Furthermore, the kinetics of depolarization-induced I_{CLCA} activation were not modified after Al^{3+} exposure and washout (Fig. 5A). Finally, Al^{3+} failed to inhibit the preactivated Cl^- conductance at 0 mV (Fig. 5B). Similar inhibitory effects on I_{CLCA} activation were also obtained with 1 mM La^{3+} and Gd^{3+}, although at this concentration the effect was poorly reversible (data not shown). La^{3+} and Gd^{3+}

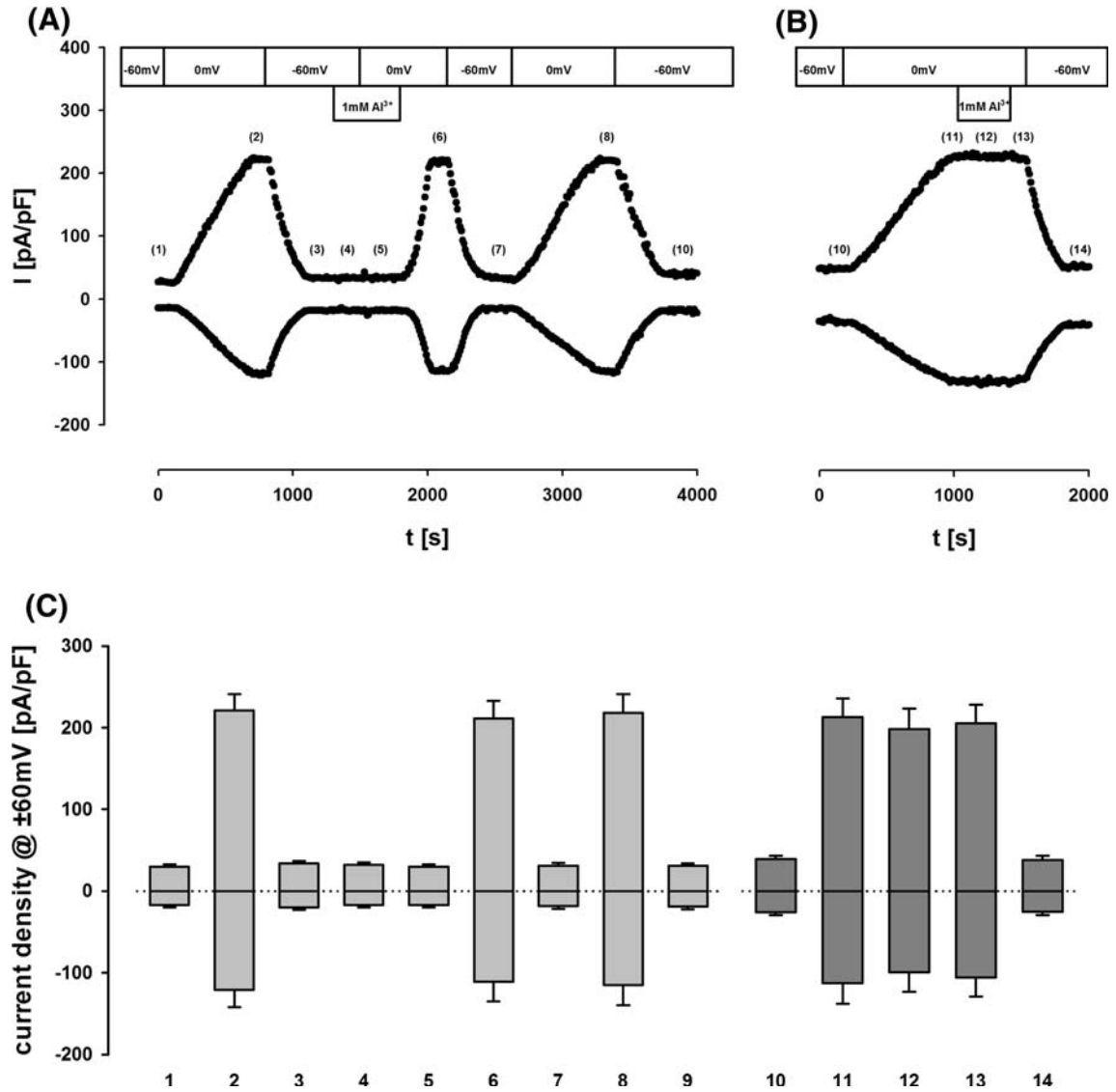

Fig. 5 Al^{3+} blocks the depolarization-activated whole-cell currents in mIMCD-3 cells. **A** Individual record of whole-cell current (perforated patch) in an mIMCD-3 cell. Membrane holding potential (V_{hold}) is indicated in the upper bars, and current at ± 60 mV is plotted. Superfusion with 1 mM Al^{3+} at $V_{hold} = -60$ mV prior to the second activation cycle blocked activation of I_{CLCA} upon switching of V_{hold} to 0 mV. Activation occurred with a minimal delay after removal of Al^{3+} (1 mM). Final activation cycle was unchanged in comparison with pre-Al^{3+} exposure. **B** Individual record of whole-cell current (perforated patch) in an mIMCD-3 cell different from that depicted in A. Membrane holding potential (V_{hold}) is indicated in the upper bars and current at ±60 mV is plotted. Superfusion with 1 mM Al^{3+} after full activation of I_{CLCA} at $V_{hold} = 0$ mV had no effect on I_{CLCA}. **C** Mean values of whole-cell current densities obtained using the protocol illustrated in **A** and **B**. Numbers below each column correspond to specific time points in the experiments depicted in **A** or **B**. Mean data from **A** $n = 5$ experiments and **B** $n = 4$ experiments

also failed to inhibit the preactivated conductance (data not shown). We then sought direct electrophysiological evidence for a voltage-dependent Ca^{2+} influx pathway which was sensitive to Al^{3+}. To do this we used whole-cell current-clamp experiments and induced membrane depolarization by switching from the standard NaCl-rich bath solution to a KCl-rich solution (where $KCl_{in} = KCl_{out}$) but that contained an inwardly directed Ca^{2+} gradient (1 mM $[Ca^{2+}]_o$). Under such conditions the equilibrium potential (E_x) for K^+, Cl^-, and Na^+ is 0 mV, whereas E_{Ca} is very positive ($\sim$120 mV assuming an intracellular $[Ca^{2+}]$ of 100 nM).

Figure 6A shows that when the external NaCl bathing solution was switched to the KCl-rich solution, there was an initial movement of the membrane potential toward 0 mV, followed, after a delay of 20–25 s, by a marked shift in V_m, to +21 ± 5 mV ($n = 8$; $P < 0.001$ vs. 0 mV and control values). These changes in V_m are consistent with a depolarization-induced activation of a Ca^{2+}-permeable conductance. Crucially, perfusion with Al^{3+} had no effect

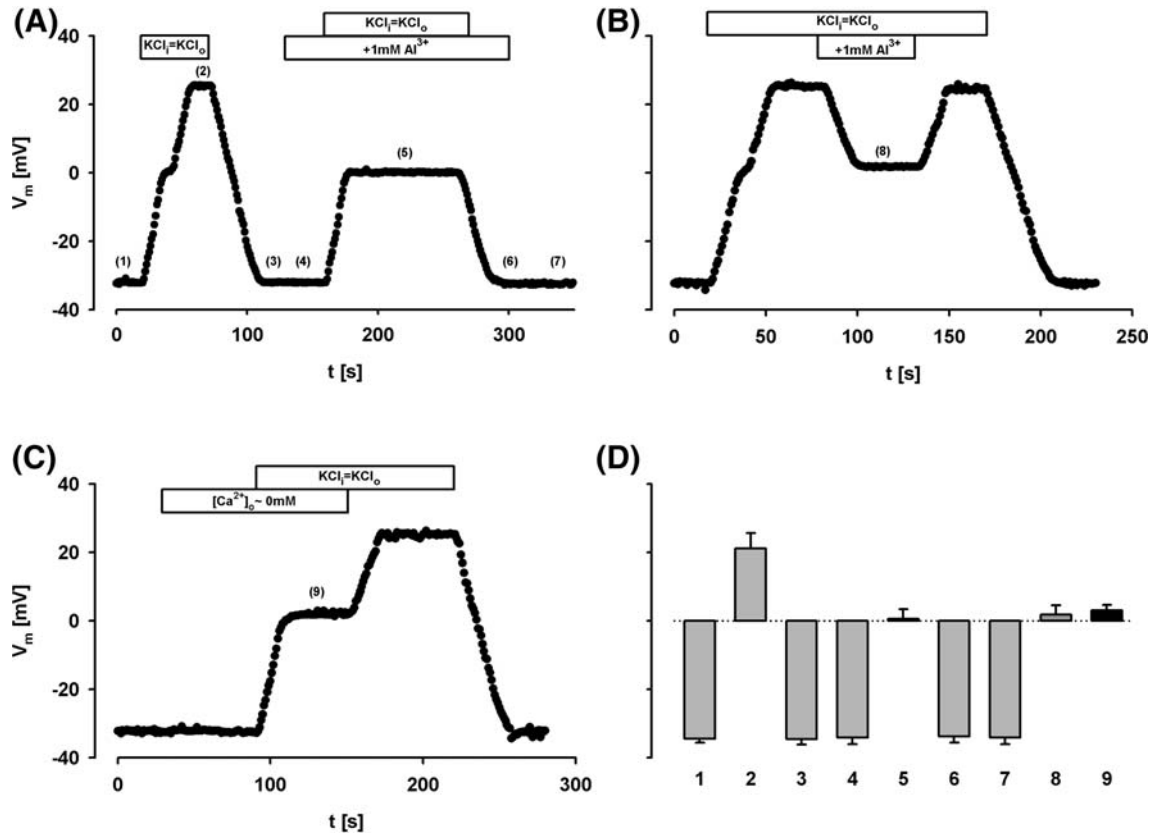

Fig. 6 Al^{3+} blocks depolarization-activated Ca^{2+} conductance. **A** Individual record of cell membrane potential (V_m) at zero holding current measured in current-clamp mode. Initially the cell was bathed in the standard NaCl-rich bath solution. This was then changed to a KCl-rich bath solution (indicated as $KCl_i = KCl_o$), which caused V_m to depolarize to ~0 mV. However, after the short delay of ~20 s, V_m shifted to ~+22 mV and remained at this value until KCl was replaced with the standard NaCl-rich solution, which caused a repolarization to initial values (approx. −35 mV). This protocol was repeated, but in this case 1.0 mM $AlCl_3$ was included in the bath solutions (both NaCl rich and KCl rich) (see Methods). In this case the KCl-rich bath solution still caused the initial depolarization to 0 mV, but the secondary depolarization was absent. **B** Repeat of the protocol depicted in A, but this time Al^{3+} was added during the secondary depolarization. **C** Experiment showing that a nominally calcium-free bath solution has no effect on the depolarization to ~0 mV induced by a KCl-rich bath solution, but it does prevent the secondary depolarization observed in calcium-containing solutions. **D** Mean V_m values obtained using the protocol illustrated in **A**–**C**. Numbers below each column correspond to specific time points in the experiments depicted in **A**–**C**. Mean data from **A** $n = 8$ experiments, **B** $n = 5$ experiments, and **C** $n = 5$ experiments

on V_m under control conditions, but abolished the establishment of a positive V_m upon switching to the KCl-rich bath solution (Fig. 6A, second part) (V_m under these conditions was not significantly different from zero, at 0.6 ± 2.8 mV; P = ns, $n = 6$). In addition, application of Al^{3+} *after* depolarization activation of the Ca^{2+} influx pathway (Fig. 6B) caused V_m to return to ~0 mV (V_m changed from +22 ± 4 to 2 ± 3 mV; $n = 5$), indicating that, once activated, the calcium influx pathway is still sensitive to Al^{3+} block. The establishment of a positive V_m upon switching to the KCl-rich bath solution could also be prevented by removing Ca^{2+} from the bath solution (Fig. 6C), thereby eliminating the driving force for Ca^{2+} influx ($V_m = 3 \pm 2$ mV, $n = 6$, $P < 0.05$, vs. 1 mM $[Ca^{2+}]_o$). The permselectivity of this calcium influx pathway was further investigated by replacing Ca^{2+} with different divalent cations (Ba^{2+}, Mn^{2+}, and Sr^{2+}). After KCl depolarization, V_m shifted to +23 ± 4, 5 ± 2, and 7 ± 2 mV, respectively (n = 3–5). Note that we were unable to isolate a calcium/barium-selective current under voltage-clamp conditions, precluding detailed analysis of this calcium conductance under this configuration.

Discussion

In this report we show that IMCD cells contain a depolarization-activated Ca^{2+} entry pathway that is functionally linked to the activity of a previously characterized Ca^{2+}-dependent Cl^- conductance (I_{CLCA}) (Shindo et al. 1996; Stewart et al. 2001; Linley et al. 2007). We show that at a holding potential of −60 mV, I_{CLCA} is essentially inactive, and the cell is predominantly K^+ selective. However, the Cl^-conductance slowly activates as the cell's membrane

potential is depolarized to below −40 mV, and at 0 mV, I_{CLCA} then becomes the dominant membrane conductance. Since activation of I_{CLCA} was abolished, by buffering intracellular Ca^{2+} or by blocking Ca^{2+} influx with Al^{3+}, and was also partially sensitive to extracellular Ca^{2+} removal, we conclude that depolarization-induced Ca^{2+} influx is an essential step in the activation of I_{CLCA}.

What Is the Molecular Nature of I_{CLCA} in IMCD Cells?

Our previous work on the calcium-activated chloride conductances of mouse IMCD-derived cell lines has emphasized the differences between the early and the late IMCD. In mIMCD-K2 cells (a model of the early IMCD), the calcium-activated chloride conductance displays strongly time-dependent activation kinetics at a moderate $[Ca^{2+}]_i$ and an ion permeability sequence of $I^- > Br^- > Cl^-$ (Boese et al. 2000, 2004), similar to the recently cloned calcium activated chloride channel TMEM16A (Caputo et al. 2008; Schroeder et al. 2008; Yang et al. 2008). In contrast, the I_{CLCA} of mIMCD-3 cells displays no time-dependent activation kinetics at any $[Ca^{2+}]_i$ level. Interestingly a number of splice variants of TMEM16A exist, one of which (TMEM16A[0]) confers a calcium-activated chloride conductance which has a reduced calcium sensitivity and no time-dependent activation kinetics, similar to the endogenous I_{CLCA} in mIMCD-3 cells (Caputo et al. 2008). TMEM16A is a member of a family of closely related proteins of unknown function, which could provide a possible reason for the apparent diversity in biophysical properties and regulation of calcium-activated Cl^- channels in different cell types.

What Is the Molecular Identity of the Al^{3+}-Sensitive Ca^{2+} Influx Pathway?

The primary site of active renal transcellular calcium reabsorption is in the distal tubule via TRPV5 (Hoenderop et al. 2005). The collecting tubule, including the medullary collecting duct, is thought not to be implicated in bulk active Ca^{2+} reabsorption due to the absence of calbindins in OMCD and IMCD. Therefore, it is likely that alternative physiological functions exist for calcium channels in these segments (Nijenhuis et al. 2003). However, it should be remembered that early studies in perfused rat IMCD did demonstrate net Ca^{2+} reabsorption (Magaldi et al. 1989), raising the possibility that apical Ca^{2+} channels in IMCD may participate in the regulation of urinary Ca^{2+} levels.

The α1G-T-type calcium channel is expressed in the IMCD and in mIMCD-3 cells (Andreasen et al. 2000) and inactivates rapidly in response to depolarizing stimuli. Since the activity of the Ca^{2+} influx pathway in mIMCD-3 cells is maintained for tens of seconds (Fig 6) under prolonged depolarization, it is unlikely that a T-type Ca^{2+} channel participates in the response reported here. L-type Ca^{2+} channels are also known to be stimulated by depolarizing membrane potentials, are inhibited by verapamil, and have been shown to be present at the mRNA level in mIMCD-3 cells (Zhao et al. 2002). Addition of verapamil, applied either acutely or during the activation process, failed to inhibit the subsequent activation of I_{CLCA} by depolarization. Therefore, it is unlikely that influx of Ca^{2+} is through L-type Ca^{2+} channels. This conclusion is supported by evidence from in vitro microperfused rat IMCD which showed no verapamil-sensitive Ca^{2+} influx (Magaldi et al. 1989). Polycystin-2 is a member of the TRPP subfamily and localizes to the plasma membrane and primary cilia of renal epithelia (Pazour et al. 2002; Yoder 2007). Polycystin-2 is equally permeable to Na^+ and K^+ but shows greater permeability to Ca^{2+} (Gonzales-Perrett et al. 2001) and is inhibited by Gd^{3+} and La^{3+} (Yoder 2007). Although I_{CLCA} activation was found to be irreversibly inhibited by Gd^{3+} and La^{3+} (data not shown), polycystin-2 channels are constitutively active at negative membrane potentials, and thus their voltage dependence makes it unlikely that they are responsible for regulating depolarization-induced activation of I_{CLCA}. The epithelial apical Ca^{2+}-influx pathway TRPV5/6 family (Cat1/ECaC) is expressed in renal tubules; TRPV6 has a distribution along the nephron that continues past the distal collecting tubule, to include the medullary collecting tubule (Nijenhuis et al. 2003; Hoenderop et al. 2005). A key feature of TRPV5/6 is that they are constitutively active at resting membrane potentials; indeed current/voltage relationships show that they are activated at hyperpolarizing potentials. More recently, Goel et al. (2007) have shown that TRPC3 and -6 are expressed in collecting duct principal cells. TRPC3 together with aquaporin 2 was present at the apical plasma membrane after stimulation with vasopressin. Importantly, this coexpression was also seen in mIMCD-3 cells, and transepithelial calcium transport in polarized layers was increased by overexpression of TRPC3 or reduced by a dominant negative TRPC3 construct (Goel et al. 2007). Similar increases in Ca^{2+} transport were seen when monolayers were stimulated with diacylgycerol analogues and with ATP, but not with thapsigargin (Goel et al. 2007). However, with all these candidate Ca^{2+} influx pathways, either the biophysical properties, the pharmacological sensitivity, or the physiological activation profile fails to identify a Ca^{2+} channel whose activity could explain our data.

Intriguingly, a mammalian homologue of the novel plant vacuolar Ca^{2+} channel AtTPC1 (Furuichi et al. 2001; Peiter et al. 2005) is highly expressed in epithelial cells of the IMCD (Ishibashi et al. 2000). Multiple-sequence alignment studies showed that the mammalian channel (TPC1) contains a well-conserved voltage sensor, which

suggests that it is likely to be voltage gated (Ishibashi et al. 2000), and in the plant *Arabidopsis thaliana*, the vacuolar Ca^{2+} channel is specifically blocked by Al^{3+} (Kawano et al. 2004; Lin et al. 2005). However, detailed information about AtTPC1 divalent selectivity is lacking. In mammals, very recent data show that hTPC1 localizes to acidic endosomes and is activated by nicotinic acid adenine dinucleotide phosphate (NAADP) (Calcraft et al. 2009). Whether TPC1 could have any role at the plasma membrane remains speculative, as no measurable membrane current was observed when exogenously expressed in either CHO-K1 cells or *Xenopus* oocytes (Ishibashi et al. 2000). Further experiments are required to determine if membrane depolarization can stimulate TPC1-containing endosomes to traffic to the plasma membrane, where TPC1 could function as the putative Al^{3+}-sensitive Ca^{2+} influx pathway described here.

Surprisingly there have been very few reports of the effect of Al^{3+} on either cloned or native Ca^{2+} channels. Busselberg et al. (1994) reported that the endogenous voltage-dependent Ca^{2+} channels of rat dorsal root ganglion neurons were sensitive to block by Al^{3+} in a manner consistent with open pore block. The permselectivity of this native channel to divalent cations has not been described in detail, although it is equally permeable to barium ions (D. Busselberg, personal communication), which is similar to our present findings. Bobkov and Ache (2005) also reported that a TRP-like, Na^{+}-activated, Ca^{2+}-permeable channel, in lobster olfactory neurons was inhibited by *intracellular* Al^{3+}, La^{3+}, and Gd^{3+} (100–200 μM), when applied to inside-out membrane patches. Those authors also stated that the three trivalent cations also inhibited single-channel activity when applied to the extracellular side of outside-out membrane patches, although no data were shown. Interestingly, block by these trivalents was not reversible without the addition of a chelating agent. This is in marked contrast to our findings, where Al^{3+} block was fully reversible. The permselectivity of the lobster trp-like channel to divalent cations (relative to the Na^{+} conductance) was Na^{+} (1.0) > Ba^{2+} (0.57) > Ca^{2+} (0.36) = Sr^{2+} (0.35) > Mg^{2+} (0.27) > Mn^{2+} (0.18) (Zhainazarov and Ache 1997), which is somewhat different from the sequence we found for the mIMCD-3 influx pathway based on current-clamp measurements (Ba^{2+} = Ca^{2+} > Sr^{2+} = Mn^{2+}).

I_{CLCA} Requires Both Membrane Depolarization and Calcium Influx for Sustained Activity

The complex activation profile of I_{CLCA} at 0 mV (Fig. 1) implies that multiple steps are involved in regulating this conductance. Although we do not yet have a complete understanding of the whole process, we believe that our results suggest the following. Depolarization to 0 mV activates calcium entry into IMCD cells via an Al^{3+}-sensitive electrogenic pathway (Fig. 6), and this event leads to the subsequent activation of I_{CLCA}. Ca^{2+} entry is likely to be localized to a region close to the plasma membrane, as we did not detect any increase in bulk $[Ca^{2+}]_i$ in Fura-2 experiments after K^{+} depolarization. Furthermore, significant activation of I_{CLCA} still occurred under nominally calcium-free conditions (Fig. 3A), suggesting either that the activation process requires little calcium to proceed or that sources of calcium other than the extracellular environment are involved and are able to sustain activation to a significant level. An alternative possibility is that Mg^{2+} can partially substitute for Ca^{2+} in sustaining I_{CLCA} activation under nominally calcium-free conditions because our bath solutions always contained 1.2 mM $MgCl_2$. However, we were unable to test this possibility because exposure of mIMCD-3 cells to a nominally calcium-free bath solution with $MgCl_2$ omitted led to the immediate activation of a large cation-selective conductance (data not shown), similar to the effect of adding EGTA (Stewart et al. 2001). However, based on our current-clamp experiments we believe that the Mg^{2+} permeability of the calcium influx pathway is not significant, since V_m did not change after KCl depolarization under nominally calcium-free conditions, despite there being a significant inwardly directed electrochemical gradient for Mg^{2+} influx in these experiments (this assumes that the free intracellular $[Mg^{2+}]$ is ~0.5 mM [Schweigel et al. 1999]).

Blocking Ca^{2+} influx with Al^{3+} prevented activation of I_{CLCA} by depolarization (Fig. 5), confirming that depolarization alone cannot activate I_{CLCA}. However, Al^{3+} only prevented I_{CLCA} activation when present *before* membrane depolarization, and the trivalent ion had no effect on the preactivated conductance (Fig. 5B), indicating that sustained Ca^{2+} influx is not required to maintain I_{CLCA} fully active under depolarized conditions. This conclusion is further supported by the current-clamp experiments, where Al^{3+} was able to block the Ca^{2+} influx pathway after activation by membrane depolarization (Fig. 6B). These results also show that Al^{3+} is not a blocker of I_{CLCA} itself. On the other hand, simply raising cytosolic Ca^{2+} to 1 μM (at a membrane potential of −60 mV) was not sufficient to cause a sustained activation of I_{CLCA} (Fig. 4). This implies that both membrane depolarization and Ca^{2+} influx are needed for sustained activity. Thus, the observed interplay among membrane voltage, Ca^{2+} influx, and I_{CLCA} activity cannot be satisfactorily explained by the direct activation of I_{CLCA} via an initial voltage-dependent Ca^{2+} influx. In addition, pre-exposure to external Al^{3+} followed by washout of Al^{3+} (at 0 mV) led to a shortening of the 'activation lag' phase and also to an increased rate of activation of I_{CLCA} at 0 mV (Fig. 5A), indicating that there are other (as yet unidentified) voltage-dependent processes

which contribute to the sustained activity of I_{CLCA} (at 0 mV + Al^{3+}). However, the quicker activation of the chloride conductance after Al^{3+} washout may also reflect unblocking of already 'activated' calcium channels. Clearly, further experiments are required to fully understand the relationship among voltage, calcium entry, and activation of I_{CLCA}.

It is also worth noting that barium could substitute perfectly for calcium in sustaining I_{CLCA} activity. This therefore suggests that I_{CLCA} is activated by barium, as well as calcium. Although there are few examples where this has been directly tested for other Ca^{2+}-activated Cl^-channels, Yuan (1997) showed that Ba^{2+} did not support Ca^{2+}-activated Cl^- currents in pulmonary smooth muscle cells. This suggests that I_{CLCA} is in fact not directly activated by calcium, but the process of activation requires this divalent cation. Because Ba^{2+} can replace Ca^{2+} during exocytosis (Neves et al. 2001), then it is possible that a critical step in I_{CLCA} activation involves exocytosis/insertion of proteins into the plasma membrane.

Physiological Role of I_{CLCA}

The physiological importance of the coupling of a voltage-activated Ca^{2+} influx to activation of a Cl^- channel in the IMCD is uncertain. Sodium absorptive and chloride secretory pathways appear to exist in all segments of rat IMCD (Wallace et al. 2001). Cyclic AMP-mediated stimulation of IMCD both reduces transepithelial absorptive flux of Na^+ and increases secretory Cl^- flux (Rocha and Kudo 1990) via activation of CFTR (Wallace et al 2001). Amiloride-sensitive and mineralocorticoid-regulated sodium reabsorption in the rat terminal (papillary) inner medullary collecting duct in vivo was confirmed by Ullrich and Papavassiliou as early as 1979, while recent patch-clamp measurements and ENaC expression data (Frindt et al. 2007) point to hormone-regulated amiloride-sensitive ENaC currents in the rat inner medulla. Activation of CFTR in cultured murine CCD may, however, inhibit or stimulate transepithelial Na^+ absorption dependent on the electrochemical gradient for Cl^- (Chang et al 2005). Measurements of transepithelial (V_t) and basolateral (V_{bl}) voltages in isolated ex vivo rat IMCD indicate that amiloride reduces V_t from −3.0 to +1.4 mV and hyperpolarizes V_{bl} by 4.4 to −53.8 mV in this high-resistance epithelium (Stanton 1989). With such apical membrane voltages there would be only partial calcium-coupled Cl^- channel activation, as shown for mIMCD-3 (Fig. 2). However as noted by Zeidel (1993), ex vivo measurements of IMCD net Na^+ transport have often failed to match Na^+ absorption rates in vivo. Basolateral $HCO_3^-$and K^+ conductances may also depolarize V_{bl} (Stanton 1989), suggesting alternative ways to activate I_{CLCA}. In mIMCD-3 cells, ATP and Zn^{2+} stimulate transient increases in global cytosolic Ca^{2+}, which also activate I_{CLCA}, indicating that multiple regulatory pathways converge on I_{CLCA} (Stewart et al. 2001; Linley et al. 2007). The interdependence of these stimulatory pathways incorporating the unique environment of the IMCD on regulation of I_{CLCA} now needs to be investigated.

Acknowledgments We wish to thank Kidney Research for a studentship to J.E.L. J.E.L. and S.H.B. contributed equally to this work.

References

Andreasen D, Jensen BL, Hansen PB, Kwon T-H, Nielsen S, Skott O (2000) The alpha(1G)-subunit of a voltage-dependent Ca^{2+} channel is localized in rat distal nephron and collecting duct. Am J Physiol Renal Physiol 279:F997–F1005

Bean BP (1989) Classes of calcium channels in vertebrate cells. Annu Rev Physiol 51:367–384

Bertog M, Letz B, Kong W, Steinhoff M, Higgins MA, Biefeld-Ackermann A, Bunnett EW, Korbmacher C (1999) Basolateral proteinase-activated receptor (PAR-2) induces chloride secretion in M-1 mouse renal cortical collecting duct cells. J Physiol 521:3–17

Bobkov YV, Ache BW (2005) Pharmacological properties and functional role of a TRP-related ion channel in lobster olfactory receptor neurons. J Neurophysiol 93:1372–1380

Boese S, Glanville M, Aziz O, Gray MA, Simmons NL (2000) Ca^{2+} and cAMP-activated Cl^- conductances mediate Cl^- secretion in a mouse renal IMCD cell-line. J Physiol 523:325–338

Boese S, Aziz O, Simmons NL, Gray MA (2004) Kinetics and regulation of a $Ca2^+$ activated Cl^- conductance in mouse renal inner medullary collecting duct cells. Am J Renal Physiol 286:F682–F692

Busselberg D, Platt B, Michael D, Carpenter DO, Haas HL (1994) Mammalian voltage-activated calcium channels are blocked by Pb^{2+}, Zn^{2+} and Al^{3+}. J Neurophysiol 712:1491–1497

Caputo A, Caci E, Ferrera L, Pedemonte N, Barsanti C, Sondo E, Pfeffer U, Ravazzolo R, Zegarra-Moran O Galietta LJV (2008) TMEM16A, a membrane protein associated with calcium-dependent chloride channel activity. Science 322:590–594

Chang CT, Bens M, Hummler E, Boulkroun S, Schild L, Teulon J, Rossier BC, Vandewalle A (2005) Vasopressin-stimulated CFTR Cl^- currents are increased in the renal collecting duct cells of a mouse model of Liddle's syndrome. J Physiol 562:271–284

Calcraft PJ, Ruas M, Pan Z, Cheng, X, Arredouani A, Hao X, Tang J, Rietdorf K, Teboul L, Chuang K-T, Lin P, Xiao R, Wang C, Zhu Y, Lin Y, Wyatt CN, Parrington J, Ma J, Evans AM, Galione A, Zhu MX (2009) Nature. doi:10.1038/nature08030

Evans MG, Marty A (1986) Calcium-dependent chloride currents in isolated cells from lacrimal glands. J Physiol 378:437–460

Frindt G, Ergonul Z, Palmer LG (2007) Na channel expression and activity in the medullary collecting duct of rat kidney. Am J Physiol Renal Physiol 292:F1190–F1196

Furuichi T, Cunningham KW, Muto S (2001) A putative two pore channel AtTPC1 mediates Ca^{2+} flux in Arabidopsis leaf cells. Plant Cell Physiol 42:900–905

Goel M, Sinkins WG, Zuo CD, Hopfer U, Schilling WP (2007) Vasopressin-induced membrane trafficking of TRPC3 and AQ2 channels in cells of the rat renal collecting duct. Am J Physiol Renal Physiol 293:F1476–F1478

Gonzales-Perrett S, Kim K, Ibarra C, Damiano AE, Zotta E, Batelli M, Harris PC, Reisin IL, Arnaout MA, Cantiello HF (2001) Polycystin-2, the protein mutated in autosomal dominant polycystic kidney disease (ADPKD) is a calcium permeable nonselective cation channel. Proc Natl Acad Sci USA 98:790–792

Hoenderop JG, Nilius B, Bindels RJ (2005) Calcium absorption across epithelia. Physiol Rev 85:373–422

Ishibashi K, Suzuki M, Imai M (2000) Molecular cloning of a novel form (two-repeat) protein related to voltage-gated sodium and calcium channels. Biochem Biophys Res Commun 270:370–376

Kawano T, Kadano T, Fumoto K, Lapeyrie F, Kuse M, Osobe M, Furuichi T, Muto S (2004) Aluminum as a specific inhibitor of plant TPC1 Ca^{2+} channels. Biochem Biophys Res Commun 324:40–45

Kose H, Simmons NL, Brown CDA (1997) Bradykinin stimulates chloride secretion in an inner medullary collecting duct cell line (mIMCD-3). J Physiol 504:140

Kose H, Boese SH, Glanville M, Gray MA, Brown CDA, Simmons NL (2000) Bradykinin regulation of salt transport across mouse inner medullary collecting duct epithelium involves activation of a Ca^{2+}-dependent Cl^{-} conductance. Br J Pharmacol 131:1689–1699

Lin C, Yu Y, Kadano T, Iwata M, Umemura K, Furuichi T, Kuse M, Isobe M, Yamamoto Y, Matsumoto H, Yoshizuka K, Kawano T (2005) Action of aluminium, a novel TPC1-type channel inhibitor, against salicylate-induced and cold-shock-induced calcium influx in tobacco BY-2 cells. Biochem Biophys Res Commun 332:823–830

Linley JE, Simmons NL, Gray MA (2007) Extracellular zinc stimulates a calcium-activated chloride conductance through mobilisation of intracellular calcium in renal inner medullary collecting duct cells. Pflugers Arch 453:487–495

Magaldi AJ, van Baak AA, Rocha AS (1989) Calcium transport across rat inner medullary collecting duct perfused in vitro. Am J Physiol 257:F738–F745

Neves G, Neef A, Lagnado L (2001) The actions of barium and strontium on exocytosis and endocytosis in the synaptic terminal of goldfish bipolar cells. J Physiol 535(3):809–824

Nijenhuis T, Hoederop JG, van der Kemp AW, Bindels RJ (2003) Localization and regulation of the epithelial Ca^{2+} channel TRPV6 in the kidney. J Am Soc Nephrol 14:2731–2740

Pazour GJ, San Augustin JT, Follit JA, Rosenbaum JL, Witman GB (2002) Polycystin-2 localizes to kidney cilia and the ciliary level is elevated in orpk mice with polycystic kidney disease. Curr Biol 12:R378–R380

Peiter E, Maathuis FJ, Mills LN, Knight H, Pelloux J, Hetherington AM, Sanders D (2005) The vacuolar Ca^{2+}-activated channel TPC1 regulates germination and stomatal movement. Nature 434:404–408

Rauchman MI, Nigam SK, Delpire E, Gullans SR (1993) An osmotically tolerant inner medullary collecting duct cell line from an SV40 transgenic mouse. Am J Physiol 265:F416–F424

Rocha AS, Kudo LH (1990) Factors governing sodium and chloride transport across the inner medullary collecting duct. Kidney Int 38:654–666

Schroeder BC, Cheng T, Jan YN, Jan LY (2008) Expression cloning of TMEM16A as a calcium-activated chloride channel subunit. Cell 134:1019–1029

Schweigel M, Lang I, Martens H (1999) Mg^{2+} transport in sheep rumen epithelium: evidence for an electrodiffusive uptake mechanism. Am J Physiol Gastrointest Liver Physiol 277:G976–G982

Shindo M, Simmons NL, Gray MA (1996) Characterization of whole cell chloride conductances in a mouse inner medullary collecting duct cell line mIMCD-3. J Membr Biol 149:21–31

Stanton BA (1989) Characterization of apical and basolateral membrane conductances of rat inner medullary collecting duct. Am J Physiol Renal Physiol 256:F862–F868

Stewart GS, Glanville M, Aziz O, Simmons NL, Gray MA (2001) Regulation of an outwardly rectifying chloride conductance in renal epithelial cells by external and internal calcium. J Membr Biol 180:49–64

Ullrich KJ, Papavassiliou F (1979) Sodium reabsorption in the papillary collecting duct of rats. Pflugers Arch 379:49–52

Vandewalle A, Bens M, Duong van Huyen JP (1999) Immortalized kidney epithelial cells as tools for hormonally regulated ion transport studies. Curr Opin Nephrol Hypertens 8:581–587

Wallace DP, Rome LA, Sullivan LP, Grantham JJ (2001) cAMP-dependent fluid secretion in rat inner medullary collecting ducts. Am J Physiol Renal Physiol 280:F1019–F1029

Yang YD, Cho H, Koo JY, Tak MH, Cho Y, Shim WS, Park SP, Lee J, Lee B, Kim B-M, Raouf R, Shin YK, Oh U (2008) TMEM16A confers receptor-activated calcium-dependent chloride conductance. Nature 455:1210–1215

Yoder BK (2007) Role of primary cilia in the pathogenesis of polycystic kidney disease. J Am Soc Nephrol 18:1381–1388

Yuan XJ (1997) Role of calcium-activated chloride current in regulating pulmonary vasomotor tone. Am J Physiol Lung Cell Mol Physiol 16:L959–L968

Zeidel ML (1993) Hormonal regulation of inner medullary collecting duct sodium transport. Am J Physiol Renal Physiol 265:F159–F173

Zhainazarov AB, Ache BW (1997) Gating and conduction properties of a sodium-activated cation channel from lobster olfactory receptor neurons. J Membr Biol 156:173–190

Zhao PL, Wang XT, Zhang XM, Cebotaru V, Cebotaru L, Guo G, Morales M, Guggino SE (2002) Tubular and cellular localization of the cardiac L-type calcium channel in rat kidney. Kidney Int 61:1393–1406